INVESTIGATING THE ADDITIVE MANUFACTURE OF EXTRA-TERRESTRIAL MATERIALS

Athanasios Goulas*, Daniel Southcott-Engstrøm*, Ross J. Friel*, Russell A. Harris†

*Wolfson School of Mechanical, Electrical & Manufacturing Engineering, Loughborough University, Loughborough, LE11 3TU, United Kingdom
† Mechanical Engineering, University of Leeds, Leeds, LS2 9JT, United Kingdom

Abstract

The Powder Bed Fusion (PBF) additive manufacturing process category, consists of a group of key enabling technologies allowing the fabrication of both intrinsic and complex structures for a series of applications, including aerospace and astronautics. The purpose of this investigation was to explore the potential application of in-space additive manufacturing/3D printing, for onsite fabrication of structures and parts, using the available extra-terrestrial natural resources as feedstock. This study was carried out by using simulants of terrestrial origin, mimicking the properties of those respective materials found extra-terram (in space). An investigation was conducted through material characterisation, processing and by powder bed fusion, and resultant examination by analytical techniques. The successful realisation of this manufacturing approach in an extra-terrestrial environment could enable a sustainable presence in space by providing the ability to build assets and tools needed for long duration/distance missions in deep space.

Introduction

Additive Manufacturing (AM) (also known as rapid manufacturing, 3D printing, etc.) consists of a group of novel production technologies that through the synergy of already well-established fabrication techniques, such as laser welding, sintering, material extrusion, CNC-machining etc., can meet challenging manufacturing requirements and deliver bespoke and highly-complex geometries that no conventional manufacturing process is able to produce. The desired geometries are built directly from CAD data into three-dimensional objects in a layer-by-layer manner, by building and combining the two-dimensional sliced cross-sections of the geometry.

Although AM has been around for more than 20 years, it is still considered as a relatively new production approach with techniques and materials being continuously developed, resulting into significantly expanding the technology's application area, including examples in medicine [1], aerospace [2] and since quite recently space [3].

AM has been suggested as a promising approach to be applied in the field of astronautics and off-world/space manufacturing via In-Situ Resource Utilisation (ISRU) due to its autonomous nature of operation [4], where appropriate robotic equipment could be shipped to the desired planetary body and manufacture various physical components [5], such as replacement parts and various other structures by exploiting the already available materials found

on site. These assets could potentially be used for a plethora of applications such as infrastructure, replacement parts and shielding against meteoroids or solar and cosmic radiation. Therefore, high-level and detailed engineering studies have to be conducted in order to explore and identify the realistic potential for AM to be implemented into such a demanding and challenging application area.

Additionally, the limited number of studies that have been conducted up to now [6–9], come with inherent disadvantages (use of additives etc.) that would raise mission costs, a rather unwanted result, known the fact that space agencies could be spending an approx. of €10,000 to transfer a mass of 1 kilogram into low earth orbit [10].

This study, represents an effort to investigate the use of powder bed fusion additive manufacturing process category, as a candidate for in-situ manufacturing of structures and physical assets, by exploiting the naturally occurring planetary resources. A PFB process with a thermal energy source was used to fuse together particulates of ceramic multicomponent materials that simulate the properties of those extra-terrestrial materials found on the Lunar and Martian surface.

Materials & Methods

Materials

This experimental study was conducted using both commercially available and research-grade simulants of terrestrial igneous origin, processed according to the manufacturers proprietary techniques to better match the characteristics of those respective materials found on the Lunar and Martian surface.

The Lunar regolith simulant JSC-1A has been characterised as crushed volcanic tuff, rich in basalt glass and silicate minerals [11] containing less material complexities (i.e. impregnations, agglutinates, etc.) as a result of not being exposed onto space weathering conditions such as meteoroids and solar/cosmic radiation [12]. The simulant was supplied by Orbitec (Orbital Technologies Inc., Colorado, USA) and developed in coordination with NASA.

The Martian simulant JSC-MARS-1 consists of weathered volcanic tuff and was chosen due to its spectral similarities to the regolith samples collected and analysed in-situ by the Martian landers' XRF and APXS analytical equipment [13–15]. The simulant was also supplied by Orbitec and despite being a replica of the local geological samples measured, it is considered as the best available simulant available until actual regolith samples are brought back to Earth.

The Jining Martian Soil Simulant (JMSS-1), developed at the Lunar and Planetary Science Research Center at the Institute of Geochemistry, Chinese Academy of Sciences, consists mainly out of mechanically crushed basalt ore, originating from Jining mountain, with minor additions of hematite and magnetite. This particular material was selected due to better matching the chemical composition, mineralogy and physical properties of the Martian regolith as compared to the other available simulants. Although this simulant provides a better representation of the material gathered and analysed by Martian landers it is important to note that it is missing several of the alteration minerals that have been previously identified (i.e.

sulphates, carbonates and clays) [16]. The following **Table 1** consists of a representation of the bulk chemistry present in both Lunar and Martian simulants and a comparison from the real samples as acquired and analysed with a variety of observational data [17].

Table 1 – *Composition (Wt%) of the major constituents in the JSC-1A, JSC-MARS-1A and JMSS-1 Lunar and Martian Regolith Simulants compared to compositional data from actual Lunar and Martian regolith samples.*

Chemical Compound	JSC-1A (Manuf. data).	Lunar Regolith - Actual (Sample 14163) [18]	JMSS-1 [16]	JSC-MARS-1A (Manuf. data).	Martian Regolith – Actual [19]
Silicon dioxide (SiO_2)	46-49	47.3	49.28	34.5 – 44	43 – 44
Titanium dioxide (TiO_2)	1-2	1.6	1.78	3 – 4	0.56 – 1.1
Aluminum oxide (Al_2O_3)	14.5 – 15.5	15	18.5 – 23.5	7 – 7.5	
Ferric oxide (Fe_2O_3)	3-4	3.4	16.00	9 – 12	16.5 – 18.5
Iron oxide (FeO)	7 – 7.5	7.4	N.A.	2.5 – 3.5	–
Magnesium oxide (MgO)	8.5 – 9.5	9	6.35	2.5 – 3.5	6 – 7
Calcium oxide (CaO)	10 – 11	10.4	7.56	5 – 6	5.6 – 5.9
Sodium oxide (Na_2O)	2.5 – 3	2.7	2.92	2 – 2.5	2.1
Potassium oxide (K_2O)	0.75 – 0.85	0.8	1.02	0.5 – 0.6	0.15 – 0.3
Manganese oxide (MnO)	0.15 – 0.20	0.2	0.14	0.2 – 0.3	N.A.
Chromium III oxide (Cr_2O_3)	0.02 – 0.06	-	N.A.	–	–
Diphosphorus pentoxide (P_2O_5)	0.6 – 0.7	0.7	0.30	0.7 – 0.9	N.A.

Experimental Methods

Manufacturing experiments were carried out on a Selective Laser Melting (SLM) machine (SLM100A, Realizer, Borchen, Germany) that utilised an YLR-50 ytterbium-doped fibre laser (IPG Photonics, Oxford, USA) operating at a central emission wavelength of $\lambda=1.064$ μm producing a Gaussian beam profile TEM_{00}. The SLM machine had a maximum indicated power output of P=50W and was also equipped with an adjustable beam expander able to focus the laser spot size from 30 – 300 μm. All processing was conducted in Argon gas inert atmosphere with an oxygen content less than 0.1%. A beam size of $\delta=80$ μm was used, together with a layer thickness

of t=150 μm that was selected according to the maximum particle size of the feedstock powder material. The powder material was sieved through a laboratory test sieve of 125 μm apertures, producing a unimodal size distribution with particles ranging from 20 to 145 μm particles and a median of 75 μm as measured via laser diffraction (Mastersizer Sirocco 2000, Malvern Instruments Ltd., UK).

A combination of optical (MA200, Nikon Instruments Europe, Netherlands) and scanning electron microscopy (TM3030 SEM, Hitachi High-Technologies Europe, GmbH, Germany) was used for the assessment of internal porosity and microstructural analysis. Internal porosity was calculated using SEM imaging of the cross-sectioned samples. Acquired micrographs were initially binarized and processed via ImageJ where porosity was calculated as a ratio of the black to white pixels corresponding to the fraction of the surface voids over the total surface. Prior to microscopy examination, samples were mount on a clear epoxy resin, ground and polished according to a suitable metallographic regime, including grinding stages with P320 – P4000 grit size silicon carbide papers and final polishing with a polishing cloth and 0.05 μm Alumina suspension.

The spectral absorbance characteristics of the used simulants were assessed via FTIR spectrometry in the visible to near-infrared (Lambda Bio 40, Perkin-Elmer, Überlingen, Germany) and far-infrared spectra (FTIR-8400S, Shimadzu, Kyoto, Japan) including the operating wavelengths of the laser systems used on-board most powder bed fusion equipment to date.

Thermal analysis was conducted via TGA (Q5000-IR, TA Instruments Inc., USA) to quantify the materials' volatility and DSC (2920 Modulated DSC, TA Instruments, USA) to identify the materials' melting temperatures. TGA and DSC techniques were performed under argon gas environment at a heating rate of 10°C·min^{-1}. The change in crystallinity as result of processing was determined via XRD (D2 Phaser, Bruker AXS, Karlsruhe, Germany) with recorded diffraction patterns from 15-100° 2theta, using a 0.01 step size and 5 second step time.

Finally, XRF spectroscopy (Orbis-PC Micro-XRF Elemental Analyser, EDAX, Mahwah, USA) was utilised to identify the change in the elemental composition after processing, where the mechanical performance of the additively manufactured samples was investigated via the Vickers micro-indentation method according to the ASTM C1327 testing standard with an automated testing machine (Struers Durascan 70, EMCOtest, Kuchl, Austria) and compression testing via the ASTM C1424 testing standard using a universal dual column testing machine fitted with a 50kN static load cell (3366, Instron, High Wycombe, UK). All mechanical testing was conducted at 23°C and 55% RH.
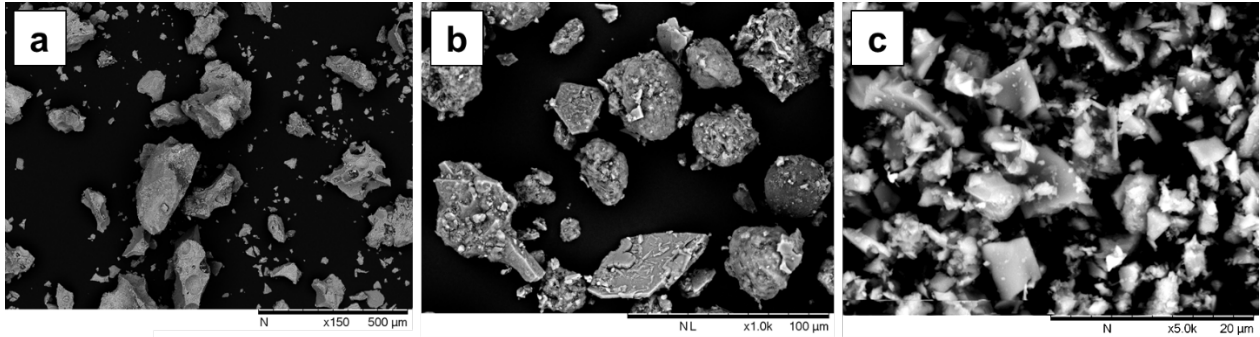
Results & Discussion

Figure 1 *– SEM images showing the particle morphology of the regolith simulants. a) JSC-1A, b) JSC-MARS-1A and c) JMSS-1.*

Investigation of the powder samples via SEM; **Figure 1**, has revealed a complex and angular morphology in all examined samples that justified the poor bed performance characteristics, such as reduced flowability and reduced packing density. Both effects are considered a common issue in most powder bed systems, especially when angular and sub-angular materials are used as feedstock, since the smooth and effective and deposition of powder layers are directly interlinked with successful inter-laminar consolidation[20].

The spectral characteristics of the powder samples are presented in **Figure 2**, where all three regolith materials have shown a highly reflective behaviour in the far-infrared spectra of 8 – 12 μm with absorbance values ranging between 10 – 25% for a wavelength of λ=10.6 μm; a typical operating wavelength of a CO_2 laser. However, the examined materials have exhibited better spectral characteristics in the visible to near-infrared spectra of 0.4 – 1.1 μm with absorbance values between 60 to 95% for a wavelength of λ=1.06 μm, that corresponds to the operating wavelength of laser systems on-board most powder bed fusion equipment. Identification of such optical characteristics were considered a necessity in order to identify the optimum processing wavelength and thus laser system, for successful fusion of the feedstock powder material.
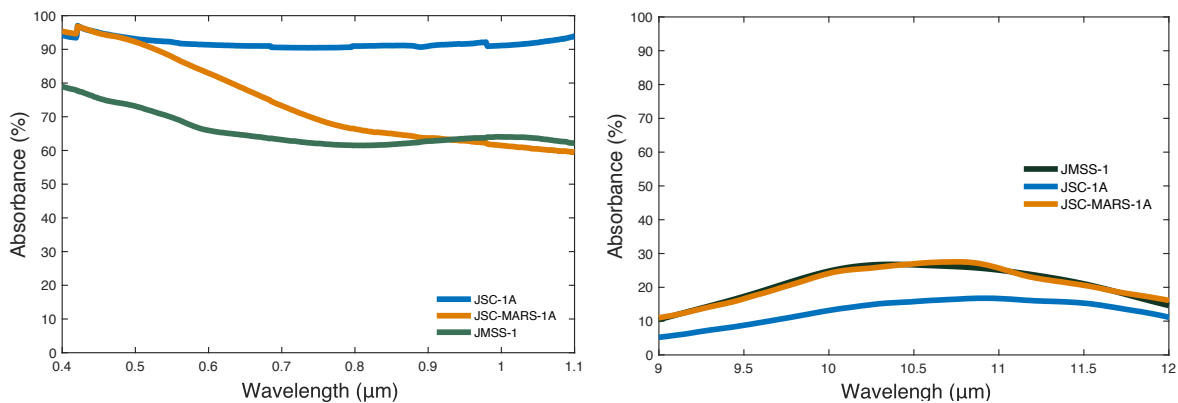

Figure 2 *- Absorbance of regolith simulants in (left) the visible to near infrared (Vis-NIR) spectra and (right) far-infrared (IR) spectra.*

The thermal behaviour of the regolith simulants was analysed via DSC and TGA; **Figure 3**. DSC data revealed a plethora of endo- and exo-thermal events associated with glass transition, crystallisation and melting behaviour. The identified glass transition temperature ranged between 600-700°C and was associated with the typical glass transition behaviour of basalt glass. The Lunar JSC-1A and Martian JSC-MARS-1A materials, showed multiple melting temperatures between 1100 – 1400°C respectively, corresponding to the melting points of their major mineral content (olivine, plagioclase, etc.). No complete melting temperature was recorded up to the equipment's maximum operating temperature, since the mineral content in the JMSS-1 has a typical melting behaviour above 1600°C.

Acquired thermograms from TGA analysis has revealed a stable thermal behaviour of both JSC-1A and JMSS-1 with a weight change of less than 1% whereas the JSC-MARS-1A material exhibited a continuous decomposition with a mass loss of up to 30% until the highest recorded temperature of 950°C. This behaviour is due to the dehydration reactions of the water content, retained in the materials crystals [19]. An inherent characteristic of the palagonitic ash, that the igneous material originates from. This latter result clearly indicates the materials non-stable thermal behaviour classifying it as rather unsuitable for powder bed fusion processing, where JSC-1A and JMSS-1 are more likely to be effectively used as feedstock due to their non-volatile performance up to the process-induced high temperatures required for material fusion.
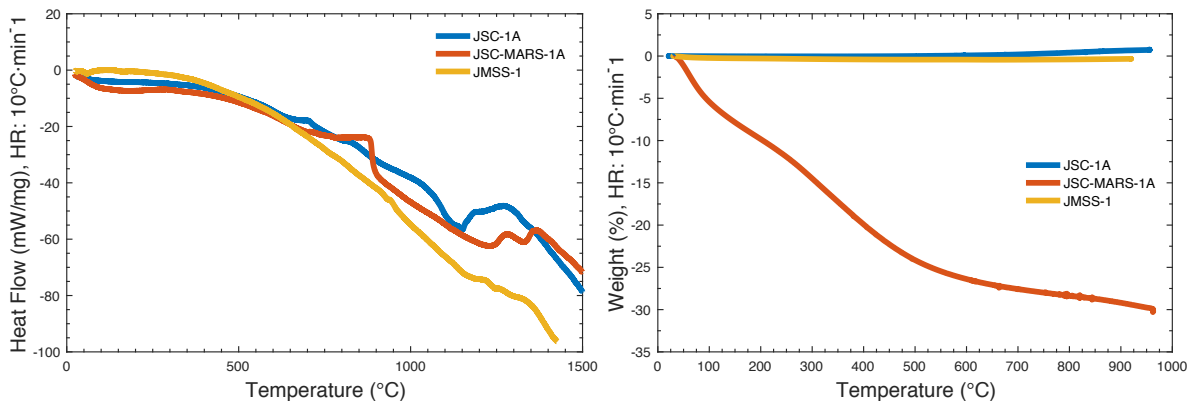

Figure 3 *– DSC (left) & TGA (right) curves overlay of Lunar and Martian Regolith Materials.*

Previous experimental studies conducted by the authors [21,22], have given a process parameter window and a laser energy density range of $0.6 – 1$ J/mm^2 where successful samples with no macroscopic defects were build using JSC-1A lunar regolith simulant. The energy density ranges of $2.4 – 4$ J/mm^2 for the JSC-MARS-1A and $0.8 – 2$ J/mm^2 for the JMSS-1 Martian regolith simulants were also identified to provide sufficient fusion between the materials' particulates. The following **Figure 4**, shows a few examples of additively manufactured parts using laser based powder bed fusion, from the JSC-1A Lunar regolith simulant.
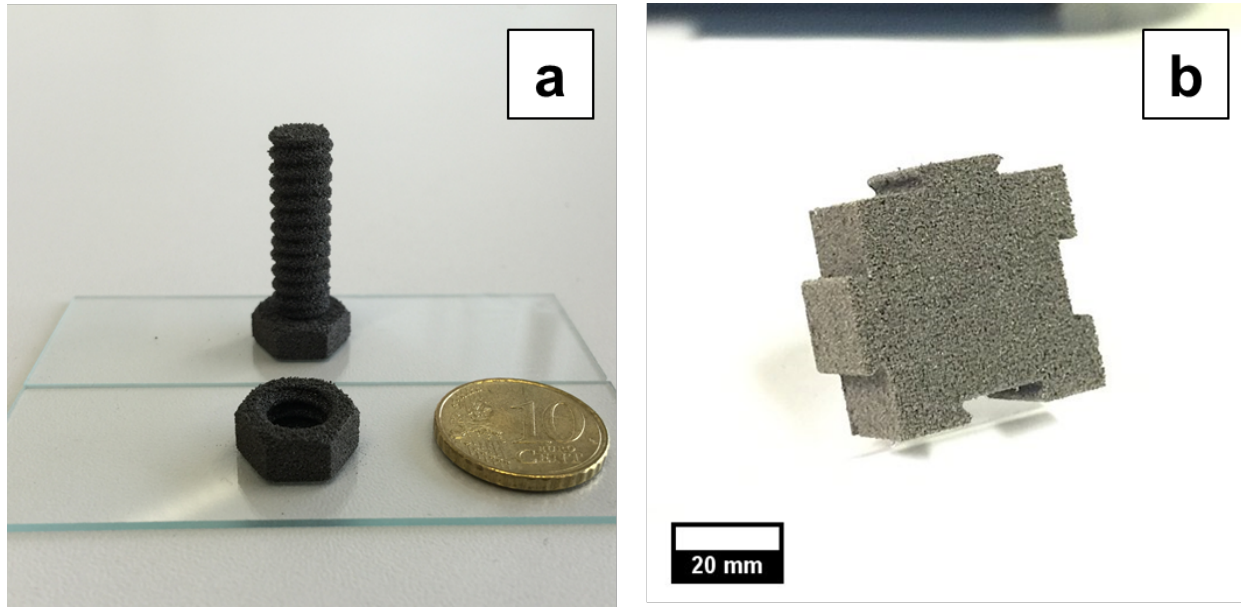
Figure 4 – Laser additively manufactured geometries from JSC-1A lunar regolith simulant. (a) M8x25 bolt with M8 nut and (b) example of a scaled down building block with mechanical interlocks.

Elemental analysis conducted via XRF prior and post processing has revealed a reduction in the elemental concentrations of the materials' constituents due to the low melting and decomposition temperatures of the mineral compounds present, as shown in **Figure 5a**. Additionally no significant difference was evident in the crystalline content of the JSC-1A lunar regolith material since major constituent crystalline phases of olivine, plagioclase and pyroxene were present before and after processing. However, the wider and less intense diffraction peaks, suggest an increase of the amorphous content due to the glass formation achieved by the very high cooling rates during processing.
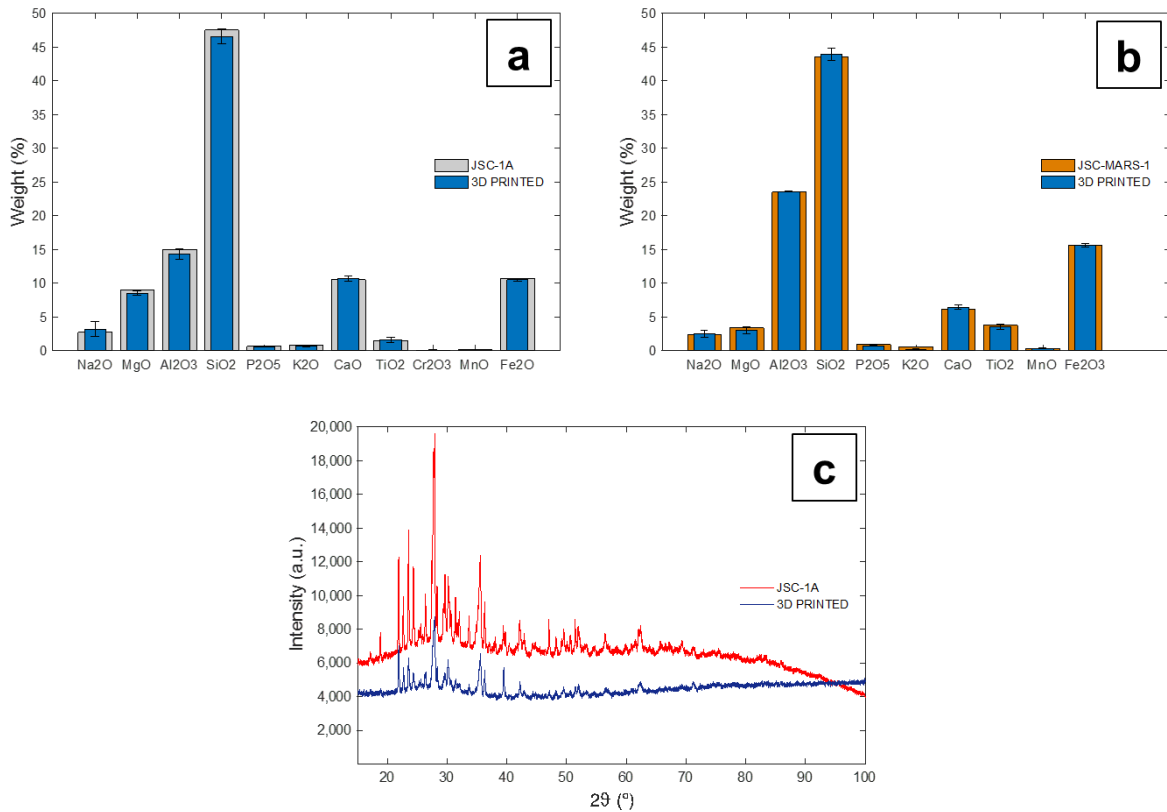
Figure 5 – Elemental concentrations prior and post processing (Wt.%) between additively manufactured Lunar (a) and Martian (b) regolith samples via XRF. And (c) diffraction patterns of Lunar regolith prior and post processing [22]

Finally, the mechanical properties of the additively manufactured lunar regolith samples, were investigated via the Vickers micro-indentation technique where the examined samples exhibited a high hardness value of 660 $HV_{0.05/15}$ which is comparable to that of soda lime glass with 545 HV, a typical glass-ceramic material used in various industrial applications. Results from compression testing revealed that the additively manufactured test samples were able to sustain compressive loads up to 350 N revealing compressive strength values of of up 3 MPa; **Figure 6**.
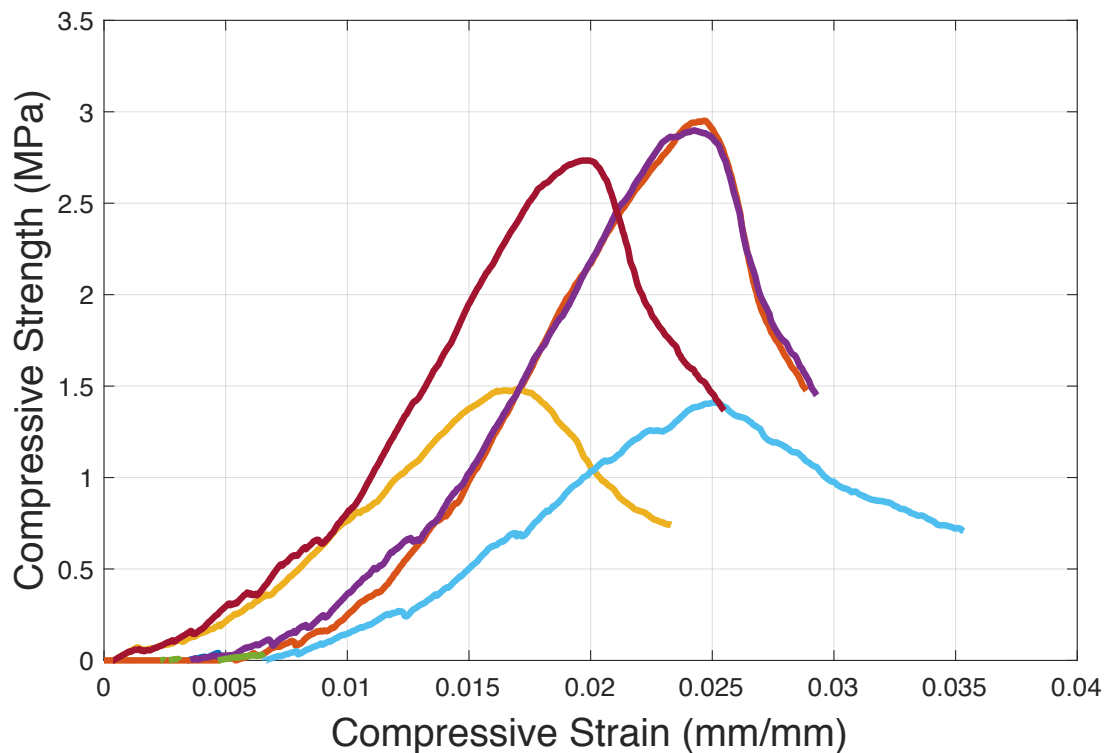
Figure 6 *- Example of typical compressive stress/strain curves recorded during compression testing experiments of additively manufactured JSC-1A test samples.*

Conclusions

This study presented an experimental investigation attempting to explore the additive manufacture of physical assets for off-word on-site manufacturing, using thermal based powder bed fusion. The study was conducted with simulants replicating the properties of those indigenous materials found off-world.

The morphological, spectral and thermal characteristics of the feedstock materials were investigated together with the mechanical properties of the fabricated structures and also the change in elemental concentration and crystallinity after processing.

Future work in this specific area would include further process optimisation by using the JMSS-1 Martian regolith simulant and also an investigation with post processing stages for improving densification towards increased mechanical performance of the additively manufactured parts from the JSC-1A Lunar regolith simulant.

Acknowledgements

References

[1]   T. Habijan, C. Haberland, H. Meier, J. Frenzel, J. Wittsiepe, C. Wuwer, C. Greulich, T. a. Schildhauer, M. Köller, The biocompatibility of dense and porous Nickel-Titanium produced by selective laser melting, Mater. Sci. Eng. C. 33 (2013) 419–426. doi:10.1016/j.msec.2012.09.008.

[2]   E.J. Wuchina, M. Opeka, Ultra-High Temperature Ceramics, 2014. doi:10.1002/9781118700853.

[3]   A.S. Keys, H.C. Morris, A.D. Sivak, M.L. Tinker, Marshall Space Flight Center Research and Technology Report 2015, 2015. http://ntrs.nasa.gov/search.jsp?R=20160006403&qs=Nm=4293224481|Subject%20Terms| ADDITIVE%20MANUFACTURING&N=4294964374.

[4]   K.R. Avchare, A. Tarwani, D. Jain, U. Saini, R. Purohit, Space manufacturing Techniques : A Review, Int. J. Sci. Res. Publ. 4 (2014) 1–10.

[5]   R.P. Mueller, S. Howe, D. Kochmann, H. Ali, C. Andersen, H. Burgoyne, W. Chambers, R. Clinton, X. De Kestellier, K. Ebelt, S. Gerner, D. Hofmann, K. Hogstrom, E. Ilves, A. Jerves, Automated Additive Construction (AAC) for Earth and Space Using In-situ Resources, in: Proc. Fifteenth Bienn. ASCE Aerosp. Div. Int. Conf. Eng. Sci. Constr. Oper. Challenging Environ. (Earth Sp. 2016), American Society of Civil Engineers, Reston, Virginia, USA., 2016. http://oro.open.ac.uk/id/eprint/45865.

[6]   B. Khoshnevis, M. Bodiford, Lunar contour crafting—a novel technique for ISRU-based habitat development, in: 43rd AIAA Aerosp. …, 2005: pp. 1–12. http://arc.aiaa.org/doi/pdf/10.2514/6.2005-538 (accessed September 4, 2014).

[7]   F. Ceccanti, E. Dini, X. De Kestelier, V. Colla, L. Pambaguian, 3D printing technology for a moon outpost exploiting lunar soil, in: 61st Int. Astronaut. Congr. Prague, CZ, IAC-10-D3, 2010: pp. 1–9. http://www.spacerenaissance.org/projects/LHD/Praga_Conference_Luna.pdf (accessed September 4, 2014).

[8]   T. Sik Lee, J. Lee, K. Yong Ann, Manufacture of polymeric concrete on the Moon, Acta Astronaut. 114 (2015) 60–64. doi:10.1016/j.actaastro.2015.04.004.

[9]   S. Sen, C.S. Ray, R.G. Reddy, Processing of lunar soil simulant for space exploration applications, Mater. Sci. Eng. A. 413–414 (2005) 592–597.

[10] Futron Corporation, Space Transportation Costs: Trends in Price Per Pound to Orbit 1990-2000, Whitepaper. (2002).

[11] P. Carpenter, L. Sibille, G.P. Meeker, S. a Wilson, Characterization Summary of JSC-1AF Lunar Mare Regolith Simulant, in: NIST Part. Work., 2006: p. 9. http://www.orbitec.com/store/JSC-1AF_Characterization.pdf.

[12] D.L. Rickman, S.A. Wilson, M.A. Weinstein, D.B. Stoeser, J.E. Edmunson, On the Manufacture of Lunar Regolith Simulants, NASA TM. TM-2013-21 (2013) 74.

[13] C.C. Allen, R. V. Morris, M.J. Karen, D.C. Golden, M.M. Lindstrom, J.P. Lockwood,

Martian Regolith Simulant JSC-Mars-1, in: Lunar Planet. Sci. Conf. XXIX, 1998: p. 1690.

[14]   C.C. Allen, K.M. Jager, R. V. Morris, D.J. Lindstrom, M.M. Lindstrom, J.P. Lockwood, Martian soil stimulant available for scientific, educational study, Eos, Trans. Am. Geophys. Union. 79 (1998) 405–405. doi:10.1029/98EO00309.

[15]   B. Bonin, Extra-terrestrial igneous granites and related rocks: A review of their occurrence and petrogenesis, Lithos. 153 (2012) 3–24. doi:10.1016/j.lithos.2012.04.007.

[16]   X. Zeng, X. Li, S. Wang, S. Li, N. Spring, H. Tang, Y. Li, J. Feng, JMSS-1: a new Martian soil simulant, Earth, Planets Sp. 67 (2015) 72. doi:10.1186/s40623-015-0248-5.

[17]   T.L. Roush, Infrared optical properties of Mars soil analog materials: Palagonites, Lunar Planet. Inst. (1993) 32–33. http://adsabs.harvard.edu/abs/1993chwe.work...32R.

[18]   R. V. Morris, R. Score, C. Dardano, G.H. Heiken, Handbook of Lunar Soils, (1983) 1183.

[19]   C.C. Allen, R. V. Morris, M.J. Karen, D.C. Golden, M.M. Lindstrom, J.P. Lockwood, MARTIAN REGOLITH SIMULANT JSC MARS-1, in: Lunar Planet. Sci. Conf. XXIX, 1998: p. 1690.

[20]   G. Strano, L. Hao, R.M. Everson, K.E. Evans, Surface roughness analysis, modelling and prediction in selective laser melting, J. Mater. Process. Technol. 213 (2013) 589–597. doi:10.1016/j.jmatprotec.2012.11.011.

[21]   A. Goulas, R.J. Friel, 3D printing with moondust, Rapid Prototyp. J. 22 (2016). doi:10.1108/RPJ-02-2015-0022.

[22]   A. Goulas, R.A. Harris, R.J. Friel, Additive manufacturing of physical assets by using ceramic multicomponent extra-terrestrial materials, Addit. Manuf. 10 (2016) 36–42. doi:10.1016/j.addma.2016.02.002.